Dark Current Mechanisms in Amorphous Selenium Avalanche Radiation Detectors

S.-A. Imam and M. Z. Kabir

Department of Electrical and Computer Engineering, Concordia University,
1455 Blvd. de Maisonneuve W., Montreal, QC, H3G 1M8, Canada, kabir@encs.concordia.ca

ABSTRACT

A theoretical model for describing bias-dependent dark current in amorphous selenium (a-Se) avalanche detector structures has been developed. The analytical model considers bulk thermal generation current from mid-gap states and carrier injection from the electrodes incorporating avalanche multiplication. An analytical expression for the multiplication factors for various current components at the avalanche fields is derived. The nature and relative importance of the injection and thermal generation currents are examined in this paper.

Keywords: Amorphous selenium, avalanche detectors, dark current, carrier injections and thermal generation.

1 INTRODUCTION

More than two decades of extensive research on amorphous selenium (a-Se) based direct conversion X-ray detectors (the incident X-rays are directly converted to electron and hole pairs, EHPs, in the photoconductor layer) have led to their use in recently commercialized flat-panel digital mammography [1]. These detectors are also presently under vigorous research endeavors for general radiography and fluoroscopy applications [2]. A-Se is currently the only commercially viable X-ray photoconductor in direct conversion detectors because of its uniform large area deposition, low dark current, and good carrier transport properties [2]. However, the a-Se detector is not perfect and has low conversion gain (X-ray to free EHP generation) compared to other potential photoconductors such as polycrystalline mercuric iodide or lead oxide [3]. The overall noise can be even higher than the signal strength in some parts of a-Se detectors in low dose imaging (e.g., in *fluoroscopy*) and thus severely affects the diagnostic features of the image. One extremely important attribute of a-Se is that it exhibits impact ionization, i.e., at a very high field F (above ~70-80 V/μm) holes in a-Se can gain enough energy to create new EHPs through impact ionization with useful avalanche gain of 1000 or more [4]. Thus avalanche multiplication may increase the signal strength and improve the signal to noise ratio in low dose X-ray imaging applications. However, the dark current in avalanche detectors can be high and very critical because of extremely high field and the avalanche nature of the dark current (the applied field causes a current to flow through the detector in absence of irradiation, which is called dark current). The dark current should be as small as possible since it is a source of noise, reduces the signal to noise ratio and dynamic range of the detector. It is one of the most important factors for the selection of the photoconductor and detector structure for X-ray imaging applications.

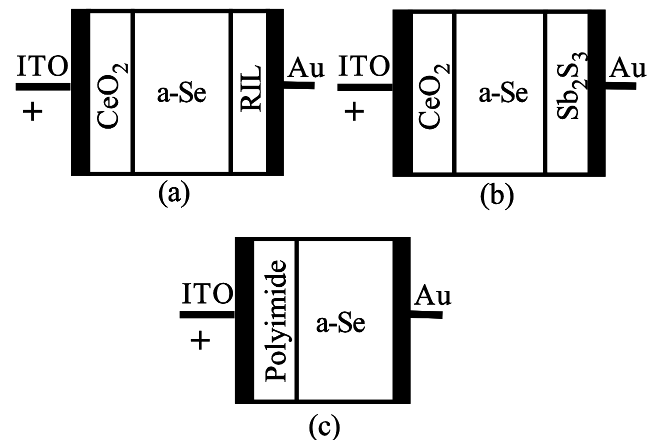

Figure 1: Schematic diagrams of a-Se avalanche detector structures with ITO top electrode; (a) Type 1: CeO_2 hole blocking and RIL electron blocking layers, and Au bottom electrode, (b) Type 2: CeO_2 hole blocking and Sb_2S_3 electron blocking layers, and Au bottom electrode, and (c) Type 3: polyimide hole blocking layer and Au bottom electrode.

The potential avalanche selenium detector structures for solid state flat-panel digital X-ray imaging are shown in Figure 1. The detector structures are classified as; Type 1: cerium dioxide (CeO_2) hole blocking and resistive interface layer (RIL) electron blocking layers, and Au bottom electrode, (b) Type 2: CeO_2 hole blocking and Sb_2S_3 electron blocking layers, and Au bottom electrode, and (c) Type 3: polyimide (PI) hole blocking layer and Au bottom electrode. The top electrode for all the structures is positively biased indium-tin-oxide (ITO). The thickness of the CeO_2 layer is ~10-30 nm. CeO_2 is an n-type wide bandgap (bandgap E_g = 3.3 eV) semiconductor [5]. PI is an insulator with a large bandgap (E_g = 7.1 eV) and blocks hole injection [6]. The thickness of the PI layer is typically ~1 μm. The RIL layer is 1 μm thick and it is a semi-

insulating polymer, namely cellulose acetate. RIL blocks electron injection and prevents gold diffusion into a-Se structure [7]. Among these three structures as illustrated in Figure 1, the Type 1 structure has shown the minimum steady-state dark current (2 pA/mm^2 at F = 60 V/μm) because of blocking of both electron and hole injections. Only holes undergo ionization process at the practical fields (70 to 120 V/μm). At the normal operating fields (less than 10 V/μm) of commercial a-Se detectors, the thermal generation current is negligible as compared to the injection currents from the metallic electrodes [8, 9]. However, the thermal generation rate can be increased exponentially with field because of Poole-Frenkel or thermally assisted tunneling effects. Therefore, both the injection and thermal generation currents should be considered to investigate the origin of dark current in a-Se avalanche detectors. In this paper, we have performed a detailed analysis on quantitative dark current contributions from bulk thermal generation and carrier injections from the electrodes incorporating avalanche multiplication. An analytical expression for the multiplication factors for various current components at the avalanche fields is derived. The nature and relative importance of the injection and thermal generation currents are examined in this paper.

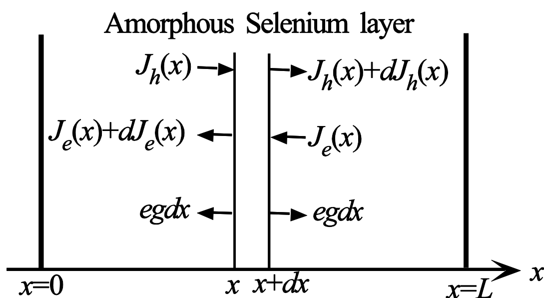

Figure 2: Avalanche multiplications of hole and electron currents under carrier injection and thermal carrier generation. L is the a-Se layer thickness.

2 THE MODEL

Suppose that hole current density per unit area $J_h(x)$ flows towards the right and electron current density $J_e(x)$ flows toward the left as shown in Figure 2. There is also a net steady-state generation of electron-hole pairs of g per unit volume per unit time from the midgap defects near the Fermi level. Assuming negligible electron multiplication, the changes of hole and electron currents in dx per unit area are,

$$dJ_h(x) = \beta J_h(x)dx + egdx \quad (1)$$

$$dJ_e(x) = -\beta J_h(x)dx - egdx \,, \quad (2)$$

where e is the elementary charge and β is the impact ionization coefficient for holes. Note that J_h in equation (2) comes from the contribution of secondary electrons due to impact ionization of holes. Considering hole injection current density J_{h0} at $x = 0$, i.e., J_h ($x = 0$) = J_{h0}, the solution of equation (1) is,

$$J_h(x) = J_{h0}\exp(\beta x) + \frac{eg}{\beta}\left[\exp(\beta x) - 1\right]. \quad (3)$$

Similarly, the solution of equation (2) is,

$$J_e(x) = J_{h0}\left[e^{\beta L} - e^{\beta x}\right] + \frac{eg}{\beta}\left[e^{\beta L} - e^{\beta x}\right] + J_{e0} \,, \quad (4)$$

where, J_{e0} is the electron injection current at $x = L$. The dark current density due to injection and steady-state bulk thermal generation is,

$$\begin{aligned} J_d &= J_h(x) + J_e(x) \\ &= J_{h0}\exp(\beta L) + \frac{eg}{\beta}\left[\exp(\beta L) - 1\right] + J_{e0} \end{aligned} \quad (5)$$

The quantity J_d can be time-dependent if the injected current densities are time-dependent. The second term in equation (5) represents the thermal generation current. Equation (5) describes the multiplication factors for thermal generation, hole and electron injection currents for the impact ionization of holes.

Once the carriers are injected into the photoconductor layer, they move by drift mechanisms (diffusion component of current is negligible compared to its drift component because of very high applied bias) [9]. Therefore, the injected current densities are [10],

$$J_{e0} = e\mu_e F n_{inj} = e\mu_e F N_C \exp\left\{-\frac{\phi_e}{kT}\right\} \quad (6)$$

And, $$J_{h0} = e\mu_h F N_v \exp\left\{-\frac{\phi_h}{kT}\right\}, \quad (7)$$

Where, n_{inj} is the average injected electron concentration from the bottom electrode, μ is the effective drift mobility, T is the absolute temperature, k is the Boltzmann constant, F ($\approx V/L$) is the applied field, V is the bias voltage, $N_{V(C)}$ is the effective density of states in the valence (conduction) band, and ϕ is the effective barrier height for injecting carriers from the electrode. The subscripts h and e stand for holes and electrons respectively. Here ϕ is an adjustable parameter.

The defect states close to the middle of the bandgap of a-Se have a high probability for thermal excitation of both types of carriers. Therefore, the steady-state thermal

generation rate is dominated by the emission from traps within kT of steady state quasi-Fermi level E_{FD}. If the excitation rates for electrons and holes are equal, E_{FD} is very close to the middle of mobility gap. The generation rate for a fully depleted sample is determined by the average carrier release time and can be written as [9, 11],

$$g = N(E_{FD})kT\omega_0 \exp\left[-\left(E_C - E_{FD} - \beta_{pf}\sqrt{F}\right)/kT\right], \qquad (8)$$

where, $N(E_{FD})$ is the density of states of a-Se at energy E_{FD} in the midgap, ω_0 is the attempt-to-escape frequency, E_{C} is the conduction band edge, $\beta_{pf} = \sqrt{e^3/\pi\varepsilon_s}$ is the Poole-Frenkel coefficient and ε_s (=$\varepsilon_0\varepsilon_r$) is the permittivity of a-Se. It is assumed in equation (8) that the density of states is constant over kT near E_{FD}.

3. RESULTS AND DISCUSSIONS

The dark current contributions from bulk thermal generation and carrier injections from the electrodes incorporating avalanche multiplication are analyzed. The effective drift mobilities are considered as the microscopic mobilities for the extremely high fields, i.e., μ_h = 0.3 cm^2/V-s and μ_e = 0.1 cm^2/V-s [12]. The parameters, L = 15 μm, ω_0 = 7 ×10^{11} /s, $N(E_{FD})$ = 10^{15} cm^{-3}eV^{-1}, ε_r = 6.7, N_C = N_V = 10^{19} /cm^3, and E_{FD} = E_g/2 are taken in all calculations [13, 14, 15]. Unless otherwise specified all the parameters mentioned above are fixed for all theoretical calculations in this paper. Other parameters such as effective barrier height (ϕ) and mid-gap density of states $N(E)$ depend on the fabrication processes and therefore, these are considered as adjustable parameters in the model. The avalanche multiplication factor highly depends on the electric field and the a-Se layer thickness. The impact ionization coefficient is taken from the experimental results of [4] and plotted in Figure 3. The impact ionization coefficient follows the relation, $\beta(F) = (1.1\times10^7) \times \exp(-1.09\times10^3/F)$ mm^{-1} by fitting with experimental data of [4]. The impact ionization starts at the electric field of 70 V/μm and increases sharply with field.

The mobility gap of a-Se varies from 2.0 eV to 2.2 eV, and the thermal generation highly depends on the mobility gap. Figure 4 shows thermal generation current density versus electric field for varying mobility gap. The thermal generation current increases by almost one order of magnitude per 0.1 eV of reduction of mobility gap. Also, the thermal generation current increases sharply with increasing electric field.

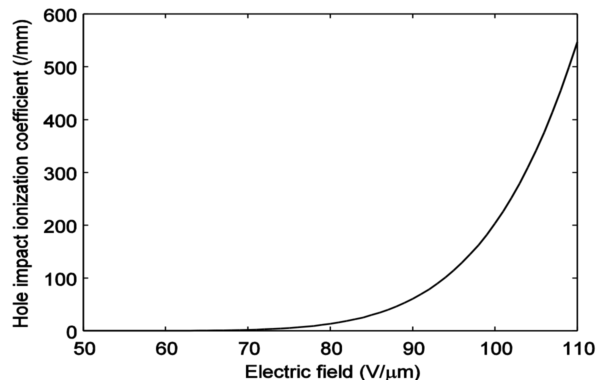

Figure 3: Impact ionization coefficient of holes as a function of electric field in a-Se.

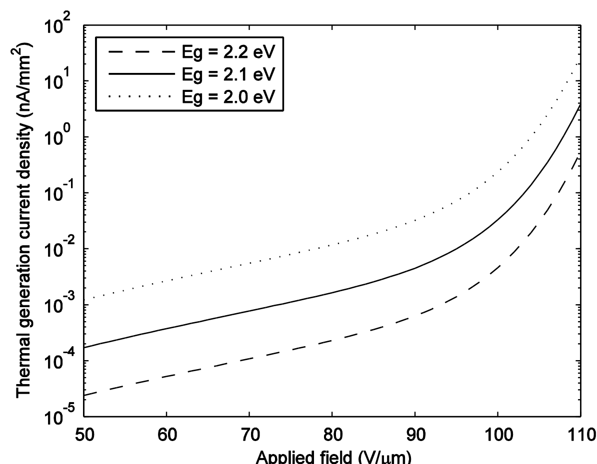

Figure 4: Thermal generation current density versus electric field for three different mobility gaps of a-Se.

The hole injection current is more critical than the electron injection current since the hole current undergoes avalanche multiplication process. Figure 5 shows the thermal generation and hole injection current densities as a function of electric field. The dotted line represents the thermal generation current density for the mobility gap of 2.1 eV. The two sets of hole injection currents are; (a) the hole injection current is equal to the thermal generation current at 50 V/μm, and (b) the injection current is 10 times higher than the thermal generation current at 50 V/μm. The effective barrier for holes from the top electrode can be much lower than the theoretical one because of many mid-gap defect levels near the valance band in dielectric hole blocking layer. The carrier transport in the dielectric hole blocking layer in Type 1&2 detectors can follow Poole-Frenkel mechanisms. The solid and dashed lines represent hole injection current without and with Poole-Frenkel emission, respectively. The rate of increase of injection

current is slower than that of thermal generation current below the avalanche threshold field (70 V/μm) but it is larger than that of thermal generation current past the avalanche threshold field. The impact of avalanche multiplication on the hole injection current is higher than that on the thermal generation current as evident from equation 5. The Poole-Frenkel effect lowers the potential barrier and enhances the injection current.

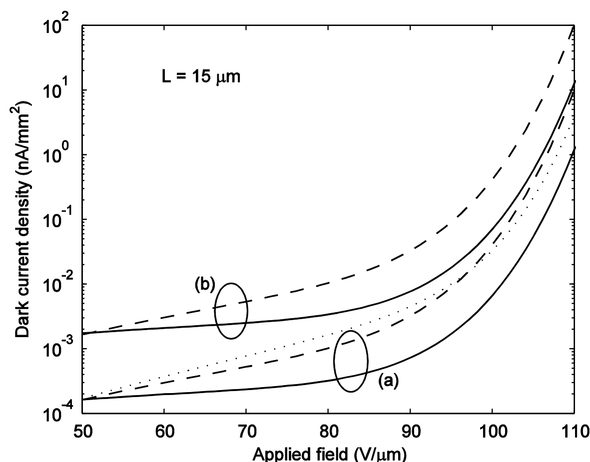

Figure 5: Hole injection current density as a function of electric field for (a) injection equals to thermal generation and, (b) injection is ten times thermal generation current at 50 V/μm. The dotted line represents the thermal generation current density for the mobility gap of 2.1 eV.

4 CONCLUSIONS

A physics-based theoretical model for describing bias-dependent steady-state dark current behavior in amorphous selenium (a-Se) avalanche detector structures has been described. An analytical expression for the multiplication factors for various current components at the avalanche fields is derived. The nature and relative importance of the injection and thermal generation currents are examined in this paper. The steady-state dark current is the minimum for the structures that have effective blocking layers for both holes and electrons.

Acknowledgement

The authors thank NSERC and Concordia University for financial support.

REFERENCES

[1] M. Z. Kabir, E. V. Emelianova, V. I. Arkhipov, M. Yunus, G. Adriaenssens, and S. O. Kasap, J. Appl. Phys., vol. **99**, pp. 124501 (2006).

[2] S. O. Kasap, J. B. Frey, G. Belev, O. Tousignant, H. Mani, J. Greenspan, L. Laperriere, O. Bubon, A. Reznik, G. DeCrescenzo, K. S. Karim and J. A. Rowlands, Sensors, vol. **11**, pp. 5112-5157 (2011).

[3] S. O. Kasap, M. Z. Kabir, and J. A. Rowlands, Curr. Appl. Phys., vol. **6**, pp. 288-292 (2006).

[4] S. O. Kasap, J. A. Rowlands, S. D. Baranovskii, and K. Tanioka, J. Appl. Phys., vol. **96**, pp. 2037-2048 (2004).

[5] K. Kikuchi, Y. Ohkawa, K. Miyakawa, T. Matsubara, K. Tanioka, M. Kubota, and N. Egami, Phys. Stat. Sol. *C,* vol. **8**, pp. 2800-2803 (2011).

[6] S. Abbaszadeh, N. Allec, S. Ghanbarzadeh, U. Shafique, and K. S. Karim, IEEE Trans. Electron Devices, vol. **59**, pp. 2403-2409 (2012).

[7] O. Bubon, G. DeCrescenzo, J. A. Raowlands and A. Reznik, J. non-cryst. Solids, vol. **358**, pp. 2431-2433 (2012).

[8] J. B. Frey, G. Belev, O. Tousignant, H. Mani, L. Laperriere, and S. O. Kasap, J. Appl. Phys., vol. **112**, pp. 014502 (2012).

[9] S. A. Mahmood and M. Z. Kabir, J. Vac. Sci. Tech. A, vol. **29**, pp. 031603 (2011).

[10] S. A. Mahmood, M. Z. Kabir, O. Tousignant, H. Mani, J. Greenspan, and P. Botka , Appl. Phys. Lett., vol. **92**, pp. 223506 (2008).

[11] R. A. Street, Appl. Phys. Lett., vol. **57**, pp. 1334 (1990).

[12] H.-Z. Song, G. J. Adriaenssens, E. V. Emelianova, and V. I. Arkhipov, Phys. Rev. B., vol. **59**, pp. 10607 (1999).

[13] A.K. Bhatnagar, K.V. Reddy and V. Srivastava, J. Phys. D: Appl. Phys., vol. **18**, pp. L149-L153 (1985).

[14] G. E. Frank-Kamennetskaya, M. D. Vorontsov, and I. P. Kalinkin, Russ. Phys. J. vol. **33**, pp. 952 (1990).

[15] M. Abkowitz, Philos. Mag. Lett., vol. **58**, pp. 53 (1988).